Mixing of Ozone at Boundary Layer Top - A Lidar Study

Ricketts, H. M. A.[1], **Vaughan, G.**[1], **Norton, E. G.**[1], **and Wareing, D. P.**[2]

[1] *Centre for Atmospheric Science, University of Manchester, Oxford Road, Manchester, M13 9PL, United Kingdom (h.ricketts@manchester.ac.uk)*

[2] *Institute of Mathematics and Physics, Aberystwyth University, Penglais, Aberystwyth, SY23 3BZ, United Kingdom*

ABSTRACT

Studies of boundary layer dynamics and entrainment were carried out using field campaign data from the mobile aerosol and ozone profiler operated by the Facility for Ground based Atmospheric Measurements (FGAM) in the United Kingdom (UK). The UK-based field campaigns investigated include the Tropospheric ORganic CHemistry experiment (TORCH) in 2003, the Convective Storm Initiation Project (CSIP) in 2005 and the Leicester Air quality Measurement Project (LAMP) in 2007. The profiler is a DIfferential Absorption Lidar (DIAL) system that operates at five wavelengths simultaneously in the near ultraviolet (266nm, 289nm, 299nm, 316nm and 355nm) and has a range between 100m and 5km, depending on the meteorological conditions. Vertical aerosol backscatter profiles were calculated and ozone profiles of the boundary layer were deduced. The error in ozone mixing ratio was +/- 3ppbv. Unlike other ozone lidars, the UFAM profiler can be run at high temporal resolutions of down to 1 minute. From these profiles it was possible to follow entrainment events and the mixing of aerosol and ozone at the top of the convective boundary layer. Case studies are presented including re-entrainment of previously detrained polluted air and development of residual layers from preceding days. The chemical and physical properties of the air parcels were looked at in greater detail using accompanying instruments at each measurement site.

1. INTRODUCTION

Ozone is a reactive gas that affect the health of the biosphere. Humans and animals as well as plants can be affected by its concentration. This extended abstract presents a mobile five wavelength lidar that measures ozone mixing ratios of the atmospheric boundary layer (ABL) and the lower troposphere. These measurements are used to understand dynamics in the ABL and their effects on ozone concentration.

2. RETRIEVAL METHODS

The Elight mobile lidar is operated by the Facility for Ground based Atmospheric Measurements (FGAM) in the United Kingdom (UK) and uses five wavelengths to obtain aerosol backscatter and ozone mixing ratio profiles of the troposphere between 75 metres and 5 kilometres above the surface. These five wavelengths are 266nm, 289nm, 299nm, 316nm and 355nm and it will be shown that using these wavelengths it is possible to retrieve ozone profiles of the atmospheric boundary layer (ABL) which is normally complicated by aerosol backscatter.

2.1. Lidar Equation

The basic equation used to describe lidar return power is the lidar equation:

$$P_r(R,\lambda) = P_0(\lambda_0)\beta(R,\lambda)dR\frac{A_r}{R^2}O(R)\eta(\lambda_0,\lambda) \times e^{\int_0^R -\alpha(r,\lambda_0)dr} e^{\int_0^R -\alpha(r,\lambda)dr} \quad (1)$$

where R is the range from the lidar, λ_0 and λ are the transmitted and received wavelength, respectively, P_r is the received power, P_0 is the transmitted power, β is the backscatter coefficient, A_r is the area of the receiving telescope, O is an overlap function, η is an efficiency value specific to the lidar and α is the extinction coefficient. Equation 1 allows for inelastic scattering (ie. $\lambda_0 \neq \lambda$), however for the lidar presented here only elastic scattering is of interest (ie. $\lambda_0 = \lambda$), so the Lidar Equation can be re-written as:

$$P_r(R) = P_0\beta(R,\lambda_0)dR\frac{A_r}{R^2}O(R)\eta(\lambda_0) \times e^{-2\int_0^R \alpha(r,\lambda_0)dr} \quad (2)$$

All of the values for this equation can be measured or calculated except α and β. They can be determined by methods as described in the following section.

2.2. Aerosol Retrieval

The method of retrieving aerosol from the lidar is the commonly adopted method presented by Fernald (1984) which is an extension of the inversion method of Klett (1981). While trying to retrieve aerosol backscatter, pre-Klett methods suffered from a rapid increase in error as range increased and signal decreased. As aerosol backscatter was retrieved from the surface upwards the method presented a greater sensitivity to low signals. Klett's method inverted the equation used and retrieved aerosol backscatter from a reference height

© Proceedings of the 8th International Symposium on Tropospheric Profiling, ISBN 978-90-6960-233-2 Delft, The Netherlands, October 2009. Editors, A. Apituley, H.W.J. Russchenberg, W.A.A. Monna

downwards, which decreased the effect of errors significantly. As the reference height could be chosen above the ABL it could generally be assumed that the aerosol concentration was negligible In his original equation, Klett did not distinguish between Rayleigh (molecular) and aerosol scattering. As these both have very different scattering mechanisms Fernald (1984) realised it was important to distinguish the two resulting in the equation:

$$\beta_1(Z) + \beta_2(Z) = \frac{X(Z)exp[-2\Delta S \int_{Z_c}^{Z} \beta_2(z)dz]}{\frac{X(Z_c)}{\beta_1(Z_c)+\beta_2(Z_c)} - 2S_1 \int_{Zc}^{Z} X(z)exp[-2\Delta S \int_{Z_c}^{z} \beta_2(z')dz']dz} \quad (3)$$

where Z is the range of the lidar, P is the backscatter power, Z_c is the reference range, $X = P(Z)Z^2$, $\Delta S = S_1 - S_2$ and S_1 and S_2 are extinction-to-backscatter ratios for aerosol and Rayleigh scattering, respectively.

2.3. Lidar Ratio

S_2 can be calculated as Rayleigh backscatterers are well-defined: $S_2 = \frac{8}{3}\pi$. Calculating S_1 (commonly referred to as the Lidar Ratio and sometimes denoted as χ)is somewhat more tricky as aerosol produces Mie scattering Mie (1908) at the wavelengths used here. To solve the Mie equation it is necessary to know the size, number concentration and composition of the aerosol which is not possible from remote measurements.

It is, however, possible to measure the Lidar Ratio by using a Raman lidar. This type of lidar exploits the fact that molecules do not only scatter light elastically, but also inelastically. By combining this fact with equation 1, it is possible to calculate the aerosol-related extinction and therefore the Lidar Ratio.

Although the lidar presented here is unable to calculate the Lidar Ratio several studies were carried out across Europe to measure Lidar Ratio as part of the EARLINET project (Bösenberg, 2003). Resulting from this two values for Lidar Ratio were chosen for the UK: marine air ($S_1 = 30sr$) and 'continental' air ($S_1 = 55sr$). While these values are not ideal, the approximation is good enough for the requirements here.

2.4. Ozone Retrieval

Using the Differential Absorption Lidar (DIAL) technique it is possible to retrieve ozone mixing ratios from backscatter profiles at different wavelengths. First presented by Schotland (1966) for water vapour the DIAL technique relates to the different absorption cross-sections of a trace gas, ie. ozone. Figure 1 shows the ozone absorption cross-section as a function of wavelength. As the wavelength decreases the ozone absorbs significantly more lidar power. The technique is based on the ratio of two Lidar Equations at different wavelengths (λ_{on} and λ_{off}) chosen to have a big difference in cross-sections. This ratio can be solved to obtain the DIAL Equation:

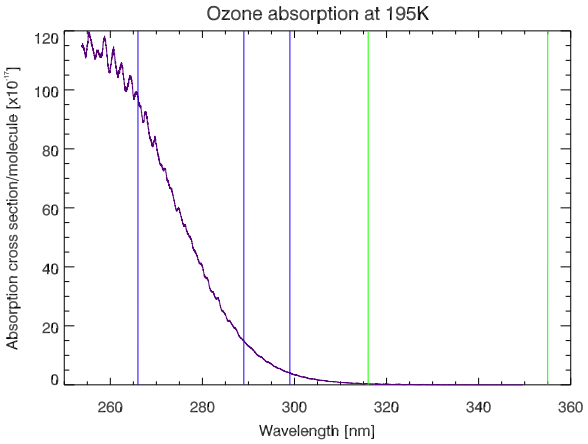

Figure 1. Ozone absorption cross-section as a function of wavelength (from Bogumil et al (2003))

$$N_{O_3}(R) = \frac{1}{2\Delta\sigma_{O_3}}\frac{d}{dR}ln\left(\frac{P_r(R,\lambda_{off})}{P_r(R,\lambda_{on})}\right) + \frac{1}{2\Delta\sigma_{O_3}}\frac{d}{dR}ln\left(\frac{\beta(R,\lambda_{on})}{\beta(R,\lambda_{off})}\right) + \frac{\alpha(R,\lambda_{off}) - \alpha(R,\lambda_{on})}{\Delta\sigma_{O_3}} \quad (4)$$

where N_{O_3} is the volume mixing ratio of ozone, σ_{O_3} is the absorption cross-section of ozone and $\Delta\sigma_{O_3} = \sigma_{O_3}(\lambda_{on}) - \sigma_{O_3}(\lambda_{off})$ is the differential absorption cross-section.

By using the correct wavelengths it is possible to use Equation 4 to retrieve ozone mixing ratio profiles. For the lidar presented here the wavelengths used in the ozone retrieval are 266nm, 289nm and 299nm.

2.5. Ångström Coefficient

The only other unknown in the DIAL Equation is the aerosol backscatter coefficient. A crude approximation would be to assume that the aerosol backscatter is constant at different wavelengths. if this were the case then the $355nm$ retrieval of aerosol backscatter coefficient could be substituted for the three ozone wavelengths. However, this approximation is inadequate as the aerosol backscatter is not wavelength-independent in the ultra-violet. The actual relationship is described with the following equation:

$$\beta_{aero}(\lambda_1)\lambda_1^{-\gamma} = \beta_{aero}(\lambda_2)\lambda_2^{-\gamma} \quad (5)$$

where γ is termed the Ångström Coefficient. In the wavelength-independent approximation mentioned above this would mean $\gamma = 0$. In the case of molecular scattering: $\gamma = 4$. For aerosol this value usually varies between 1 and 2 (Wandinger, 2004). These values were measured during EARLINET by calculating the aerosol backscatter coefficient at two different wavelengths which experience minimal trace gas absorption.

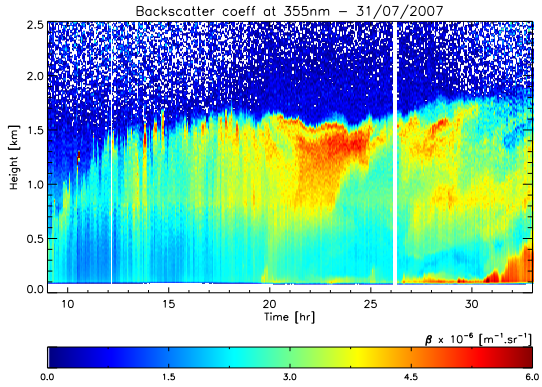

Figure 2. Aerosol backscatter coefficient retrieved from the 316nm backscatter profile for 24 hours starting at 0900UT on 31/07/2007 during the Leicester Air quality Measurement Project (LAMP)

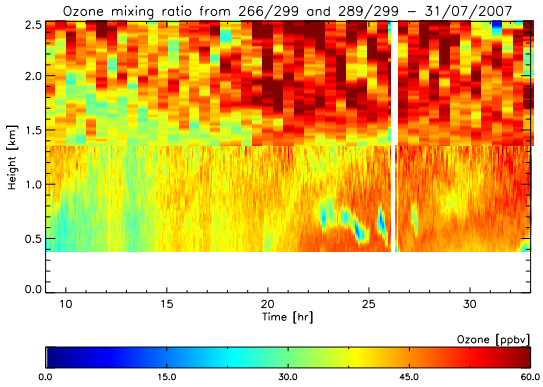

Figure 3. Ozone mixing ratio retrieved from the 266nm, 289nm and 299nm backscatter profiles for 24 hours starting at 0900UT on 31/07/2007 during the Leicester Air quality Measurement Project (LAMP)

In the case of this lidar the $316nm$ retrieval can be used as the second wavelength together with $355nm$ to derive γ. This can then be used to estimate the aerosol backscatter at the ozone wavelengths. Now the methods are described, the lidar system itself is described in the following section.

3. ELIGHT LIDAR SYSTEM

3.1. Laser

The FGAM Elight Lidar System uses five wavelengths to obtain aerosol and ozone profiles of the atmospheric boundary layer (ABL) and the lower free troposphere (FT). The five wavelengths are 266nm, 289nm, 299nm, 316nm and 355nm which are created using a powerful Nd:YAG laser which produces a 1.2J pulse at 1064nm. This pulse is then tripled and quadrupled to obtain 355nm and 266nm, respectively. The remaining three wavelengths are created using stimulated Raman scattering (SRS) by passing the 266nm beam through gas cells containing pressurised Hydrogen and Deuterium. Using the correct ratios and pressures of these gases causes inelastic scattering in the cells resulting in higher wavelength beams. Each wavelength is produced in turn, so at a laser pulse repetition frequency (PRF) of 20Hz the lidar system obtains four complete measurements every second.

3.2. Receiving Optics

The receiving telescope contains a 400mm mirror that focuses on two fields-of-view, the near and far field. The near field is focussed to allow retrievals as low as 75 metres. The far field is in focus above 500 metres and can retrieve signal backscatter up to about 10 kilometres. The light from both of these fields is collected by two separate photomultiplier tubes (PMTs) which have filters to remove solar noise. The near field filter consists of a broadband filter centred around 300nm. While this cuts out the majority of the solar noise, it also reduces the retrieval at the two extreme wavelengths, 266nm and 355nm. The far field on the other hand uses a diffraction grating to remove any unwanted wavelengths. Once correctly set up this significantly cuts down the solar noise. The PMTs are connected to 12-bit analogue-to-digital (A/D) converters which digitise the signal and then averaged over one or three minutes allowing 240 or 720 shots per profile, respectively. The data is then stored for off-line analysis.

4. RESULTS

4.1. Aerosol Backscatter

Using the algorithms presented in section 2 the data is processed for aerosol backscatter coefficient. For the aerosol retrieval the $316nm$ and $355nm$ wavelengths are used. A height of negligible aerosol is chosen to perform the inversion technique on which is generally around $3 - 4km$ and the profiles are analysed for any cloud that may interfere with the retrieval. The final dataset is a 1 minute time resolution of aerosol backscatter coefficient with a vertical resolution of 7.5 metres.

Data presented here is from the Leicester Air quality Measurement Project (LAMP) which was carried out in the summer of 2007 to understand atmospheric chemistry in the urban environment of Leicester in the UK. The day shown here is 31/07/2007 which was a clear day except for some convective cloud topping the ABL. Figure 2 shows the aerosol backscatter coefficient as retrieved from the $316nm$ beam for a 24-hour period starting at 0900UT on 31/07/2007. In this image the convective ABL is visible growing from about 500 metres when measurements began to a final height of around 1600 metres by sunset at 1959UT. The individual thermals are visible as 'domes' as are the the 'wisps' of entrained air which effectively contribute to the growth

of the boundary layer [terminology from Stull (1973)]. After sunset it is possible to see the residual layer (RL) which is the old convective boundary layer (CBL) that no longer has its convective driver at the surface and is now not in direct contact with the surface. The residual layer can be complex as different air masses advect over the site. As the skies are clear the conditions are good for a nocturnal boundary layer (NBL) to forn and this can be seen throughout the night peaking at about 100 metres which is mostly just on the border of the data coverage. The new CBL can then be seen to form on the following morning.

4.2. Ozone Mixing Ratio

By using the aerosol data from the $316nm$ and $355nm$ beams it is possible to correct for the effect of aerosol backscatter at the ozone wavelengths $266nm$, $289nm$ and $299nm$. The maximum retrieval height for ozone is about 3km, but this depends strongly on the atmospheric conditions and lidar efficiency. If the atmosphere contains high mixing ratios of ozone ($> 60ppbv$) then this can significantly decrease the maximum range. Lidar efficiency can also be variable mainly due to laser health.

On the 31/07/2007 the lidar was performing well and a maximum height of $2.5km$ was possible. Figure 3 shows the data retrieved from this day corresponding to the time in Figure 2. The data coverage of the first ozone dataset is at a time resolution of 3 minutes between 400 and 1370 metres with a vertical resolution of about 100 metres (using the far field of the 266nm/299nm wavelength pair in the DIAL retrieval) and an error of $\pm 3ppbv$. The second dataset is at a 30 minute time resolution between 1370 and 2500 metres with a vertical resolution of about 200 metres (using far field 289nm/299nm retrievals) and an error of $\pm 10ppbv$. Near field retrievals were not possible at this time due to an alignment error. Two things are worth pointing out on Figure 3.

Firstly, during the early stages of growth of the CBL (before 1200UT) it is possible to see that the ozone mixing ratios are 25ppbv in the boundary layer and 45ppbv in the free troposphere above. Also ozone mixing ratios are well-mixed in the CBL due to the convective mixing with it. As the day progresses the ozone mixing ratio in the CBL increases to 45ppbv. This ozone increase is due to the following terms in the ozone budget: flux across the boundary layer top by entrainment, photochemical production, advection and deposition. With knowledge of these four factors it would be possible to close the ozone budget. With this lidar it is possible to measure the ozone flux across the boundary layer top and for the 31/07/2007 the following values of ozone flux were calculated: $-0.54 \pm 0.27ppbv.m.s^{-1}$ during the rapid growth of the CBL before 12UT and then $-0.061 \pm 0.067ppbv.m.s^{-1}$ during the afternoon as the boundary layer is only growing slowly.

The second point of interest is the very low ozone retrievals of about 15ppbv between 2200UT and 0200UT. Current theories speculate that it is caused by a plume of nitrogen oxide (NO_x) from an emission source nearby which during the night leads to ozone destruction as it mixes with the RL air. Interestingly, Figure 2 does not show any increase in aerosol backscatter due to this plume.

5. CONCLUSIONS

In this short paper a mobile lidar was presented that can measure both aerosol backscatter and ozone mixing ratios of the atmospheric boundary layer (ABL) and lower troposphere. The algorithms used were presented and some sample data was shown. In the data is possible to use aerosol backscatter coefficient as a proxy for ABL air and then derive the entrainment rate of air in the convective boundary layer (CBL). Using the ozone mixing ratio data it is then possible to estimate the entrainment rate of ozone across the CBL top. Both aerosol and ozone data can also be used to observe the development of the residual layer (RL) during the night.

ACKNOWLEDGMENTS

I acknowledge the Natural Environment Research Council (NERC) of the United Kingdom for the PhD studentship as well as the National Centre for Atmospheric Science (NCAS) in the United Kingdom for sponsoring this research.

REFERENCES

Bogumil, K. et al., Measurements of molecular absorption spectra with the sciamachy pre-flight model: instrument characterization and reference data for atmospheric remote- sensing in the 230-2380 nm region, *Journal of Photochemistry and Photobiology a-Chemistry*, 157(2-3), pages 167184, 2003.

Bösenberg, J. et al., Earlinet: A european aerosol research lidar network to establish an aerosol climatology, *Technical report*, Max-Planck- Institut für Meteorologie, 2003.

Fernald, F. G., Analysis of atmospheric lidar observations - some comments, *Applied Optics*, 23(5), pages 652653, 1984.

Klett, J. D., Stable analytical inversion solution for processing lidar returns, *Applied Optics*, 20(2), pages 211220, 1981.

Mie, G., Beiträge zur optik trüber medien, speziell kolloidaler metallösungen, *Annalen der Physik*, 330(3), pages 377445, 1908.

Schotland, R. M., *Proc. Fourth Symp. Sensing Environment* , University of Michigan, pages 273-283 (1966).

Stull, R. B., Inversion rise model based on penetrative convection, *Journal of the Atmospheric Sciences*, 30(6), pages 10921099, 1973.

Wandinger, U., et al., Air mass modification over europe: Earlinet aerosol observations from wales to belarus, *Journal of Geophysical Research-Atmospheres*, 109(D24), 2004.